AAPG International Conference
Barcelona, Spain
September 21-24, 2003

J.I. Soto[1], M.C. Comas[1], A.R. Talukder[1] (1) Instituto Andaluz de Ciencias de la Tierra (CSIC-Granada University), Granada, Spain

Evolution of the Mud Diapirism in the Alboran Sea (Western Mediterranean)

Introduction

Mud diapirism and mud volcanism are geological phenomena that have long been known, although in recent times more emphasis has been placed on tectonic history to explain their evolution and triggering mechanisms. It is generally accepted that the emplacement of diapirs is controlled not only by the physical properties of rising materials, but also by geological events affecting the basin (e.g., Bishop 1978). Tectonic processes are the main driving mechanism invoked for the development of mud diapirism and volcanism (e.g., Higgins and Saunders 1974; Barber *et al*. 1986; Vendeville and Jackson 1992; Jackson and Vendeville 1994; Limonov *et al*. 1996; Fowler *et al*. 2000), in addition to high overpressure in sediments due to rapid sedimentation and gas generation (Hedberg 1974; Brown 1990; Reed *et al*. 1990; Hovland *et al*. 1997).

Mud diapirism and mud volcanism have been found in various tectonic settings. The majority have been reported in accretionary wedges, where the main tectonic forces are compressional, such as in the Mediterranean Ridge (Limonov *et al*. 1997; Camerlenghi *et al*. 1992; Cita *et al*. 1996; Robertson *et al*. 1996; Fusi and Kenyon 1996; Kopf *et al*. 2000, among others), Eastern Indonesia (Barber *et al*. 1986), Barbados (Martin and Kastner 1996), and Makran (Wiedicke *et al*. 2001).

The Alboran Sea basin allows mud diapirism phenomena to be studied in a different tectonic setting, since mud diapirism has existed since the middle Miocene and developed through the Cenozoic geodynamic history of the basin, typified by alternating extension and compression. Unlike the eastern Mediterranean, detailed studies of the mud diapirism in the Alboran Sea are scarce, and most of the previous works mainly refer simply to their occurrence in the basin (e.g., Bourgois *et al*. 1992; Campillo *et al*. 1992; Comas *et al*. 1992, 1999; Jurado and Comas 1992; Maldonado *et al*. 1992; Watts *et al*. 1993; Chalouan *et al*. 1997; Pérez-Belzuz *et al*. 1997).

This contribution explores in particular the geometric and possible genetic relationships between subsurface mud migration processes to feed diapir rise during the Miocene-to-Recent, and how they could be related to extensional pulses.

The mud-diapir province of the Alboran Sea

The Alboran Sea basin, behind the Gibraltar Arc -in the inner part of the Betic-Rif mountain chain (Fig. 1)- is known to be formed by crustal extension in a general Eurasian-African plate convergence setting. The direction of plate convergence was N-S between the middle Oligocene to the late Miocene and changed to NW-SE from the latest Tortonian (9-8 Ma) to the present-day (e.g. Dewey *et al*. 1989). Extension and crustal stretching in the basin were coeval with thrusting and shortening in the peripheral mountain belt from the early Miocene (about 22 Ma) to the late Tortonian (about 9-8 Ma) (among many others: Comas *et al*. 1992, 1999; García-Dueñas *et al*. 1992; Watts *et al*. 1993; Platt *et al*. 2003). Since then, contractional tectonics has produced an inversion of previous normal faults, reverse and strike-slip faults, and folding (e.g., Martínez-Martínez *et al*. 1997, 2002; Comas and Soto 1999).

Mud diapirism and associated mud volcanoes occurred only in the West Alboran Basin (WAB), developing an extensive diapir province in the major Neogene sedimentary depocentre of the basin (Fig. 1). The sedimentary cover in the WAB

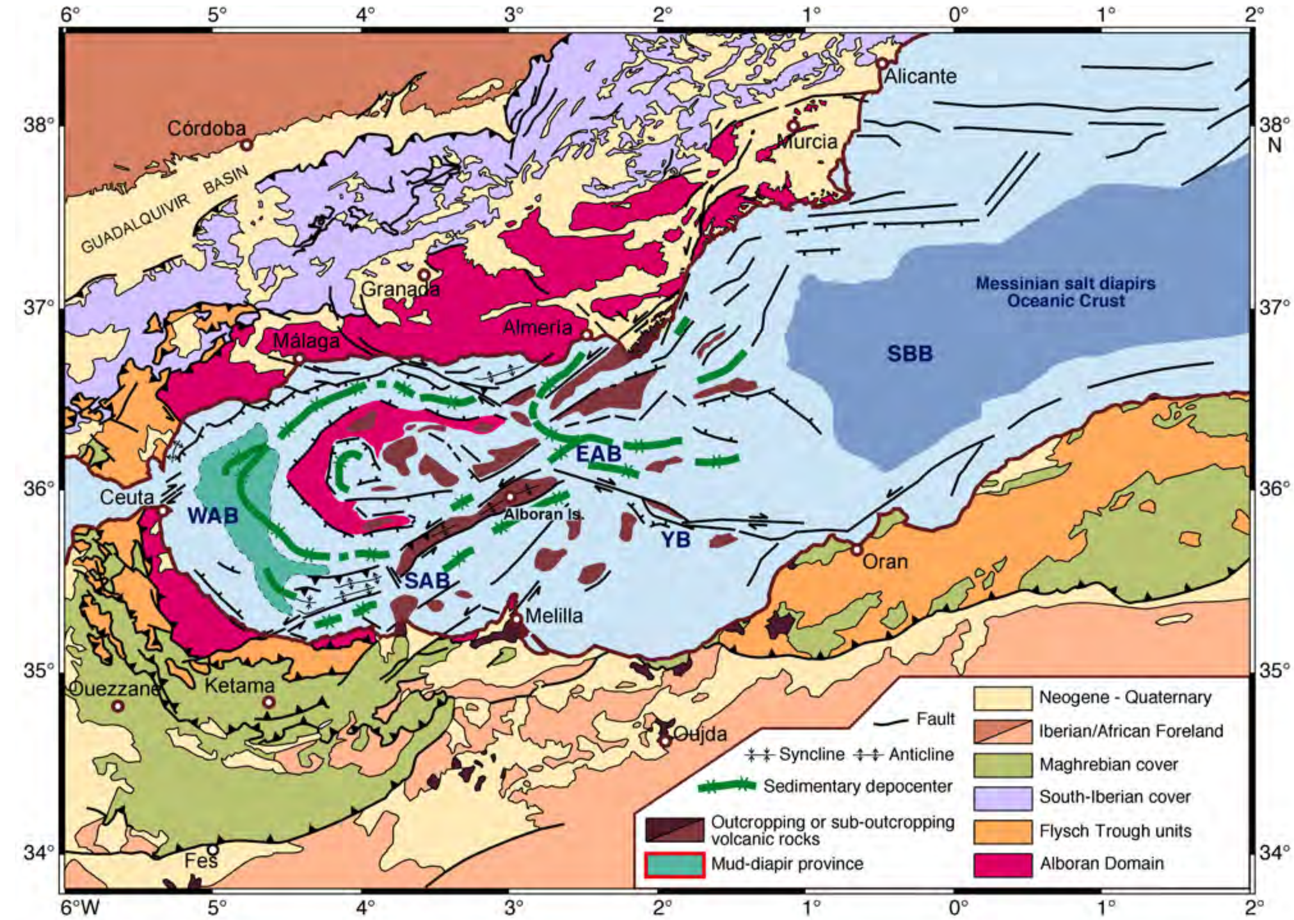

Figure 1: Tectonic map of the westernmost Mediterranean (Alboran and South Balearic seas), taken from Comas *et al*. (1999). EAB: East Alboran Basin; SAB: South Alboran Basin; SBB: South Balearic Basin; YB: Yussuf basin; WAB: West Alboran Basin. The diapir province pattern is remarked on red in the legend.

is formed of early Miocene to Quaternary deposits up to 7-9 km thick (Comas *et al*. 1992; Jurado and Comas 1992; Soto *et al*. 1996; Chalouan *et al*. 1997). According to data from commercial wells, the older deposits overlying the basement are marine sediments of latest Aquitanian (?)-Burdigalian age (Unit VI) and consist of sediments containing olistostromes, with sonic velocities and densities showing the typical features of under-compacted shales (Jurado and Comas 1992).

Major basin-wide angular unconformities within the sedimentary cover occur at the top of Unit VI (Reflector R5), at the base of Unit III (Reflector R3), and at the base of Unit I (Comas *et al*. 1992, 1999; Chalouan *et al*. 1997). Mud diapirs in the WAB have their origins in the lowermost sedimentary unit (Unit VI; Fig. 2), which is marked by high diffraction involving hyperbolic reflections and chaotic seismic facies, and probably also in the base of Unit V, that also contains undercompacted clays (Comas *et al*., 1992; Chalouan *et al*. 1997; Pérez-Belzuz *et al*. 1997). Micropalaeontological data from commercial wells indicate that Unit VI encompasses material of very different ages (from Cretaceous to Oligocene) and its age has been postulated as lower Miocene (Jurado and Comas 1992). Mud breccia samples from gravity cores in the top of the mud volcanoes also contain Eocene and upper Cretaceous clasts but the age of the mud-volcanic matrix is lower Miocene (Comas *et al*. 2000; Sautkin *et al*., 2003).

Mud diapir ascent and extension pulses during the Miocene:

The older, major stage of mud diapirism reflects the process of widespread crustal extension that affected the

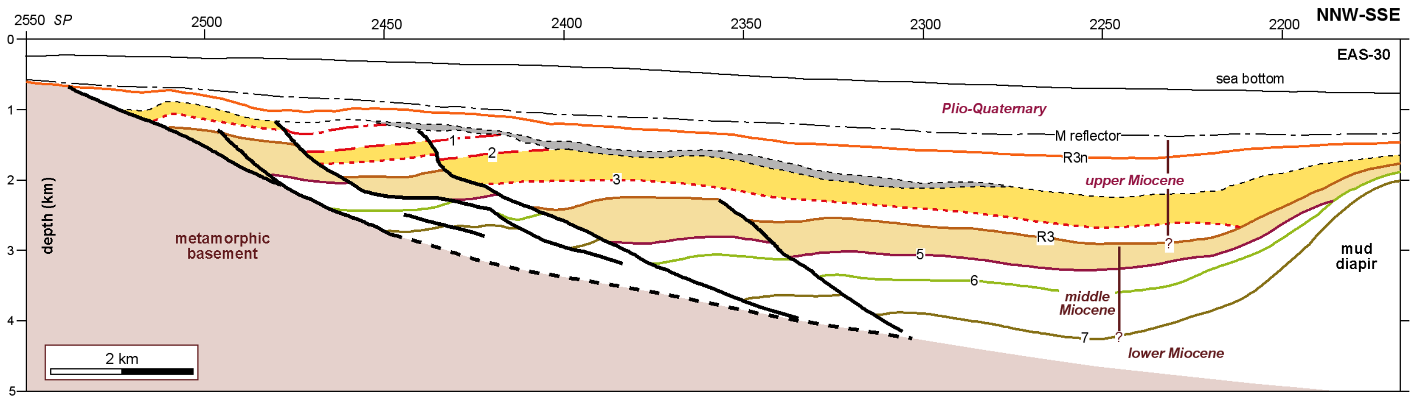

Figure 2: Depth-converted seismic line in the WAB (EAS-30) showing the general sedimentary units and major unconformities, and key geometrical relationships between extensional faults and non-piercing diapirs at the WAB.

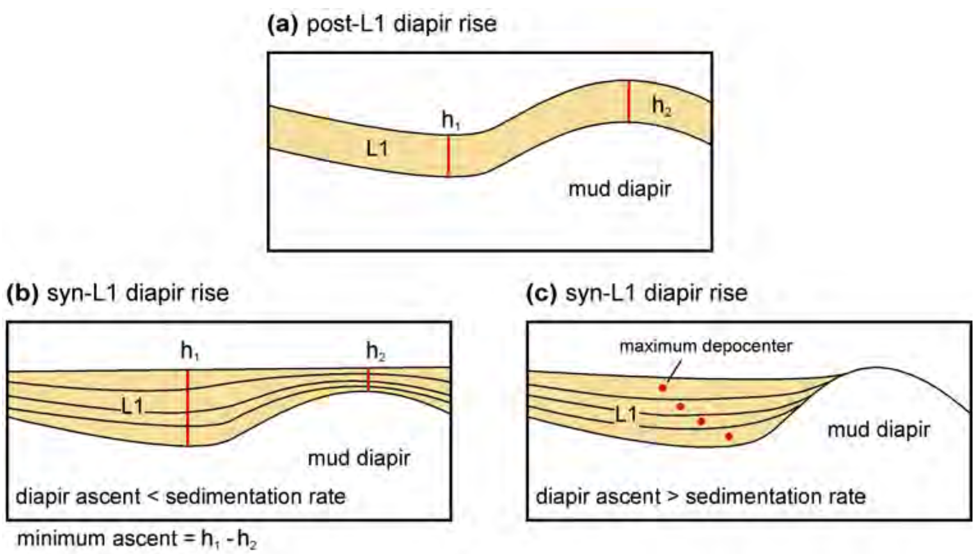

Figure 3: Diagram showing the possible relationships between a non-piercing diapir and the country sediments, and how to use these relationships (e.g. sediment thickness in the marginal through) to estimate diapir ascent rate.

Alboran basin during the middle and upper Miocene (between about 18 to 9 Ma), so mud diapirism occurred throughout the WAB depocentre for a long time. The limits of the mud diapir province run parallel to basement highs and are related to major extensional faults in the WAB (Fig. 1). Diapirism initiated on the bottom of basement half-grabens. The main extension direction is perpendicular to the axes of the mud diapir province, consistent with a W-SW extension affecting the WAB at that time (Comas and Soto 1999; Comas *et al*. 1999). The youngest stage of active diapirism is post-Messinian and developed in discrete sectors of the diapir province.

Mud diapirism started in the lower-to-middle Miocene and several distinctive major stages of activity could be identified, based on the geometrical relationships predicted in Fig. 3. If sedimentation occurred simultaneously to mud ascent at the core of a non-piercing diapir, the geometrical relationships of the nearby sedimentary units and the mud-diapir walls could be used to unravel the mud diapir history at different stages. For example, if mud ascent occurred after deposition of a sedimentary layer (L1 in Fig. 3a), the later would follow congruently the diapir high, without any significant change in thickness. If sedimentation occurred simultaneously with the diapir ascent, by the

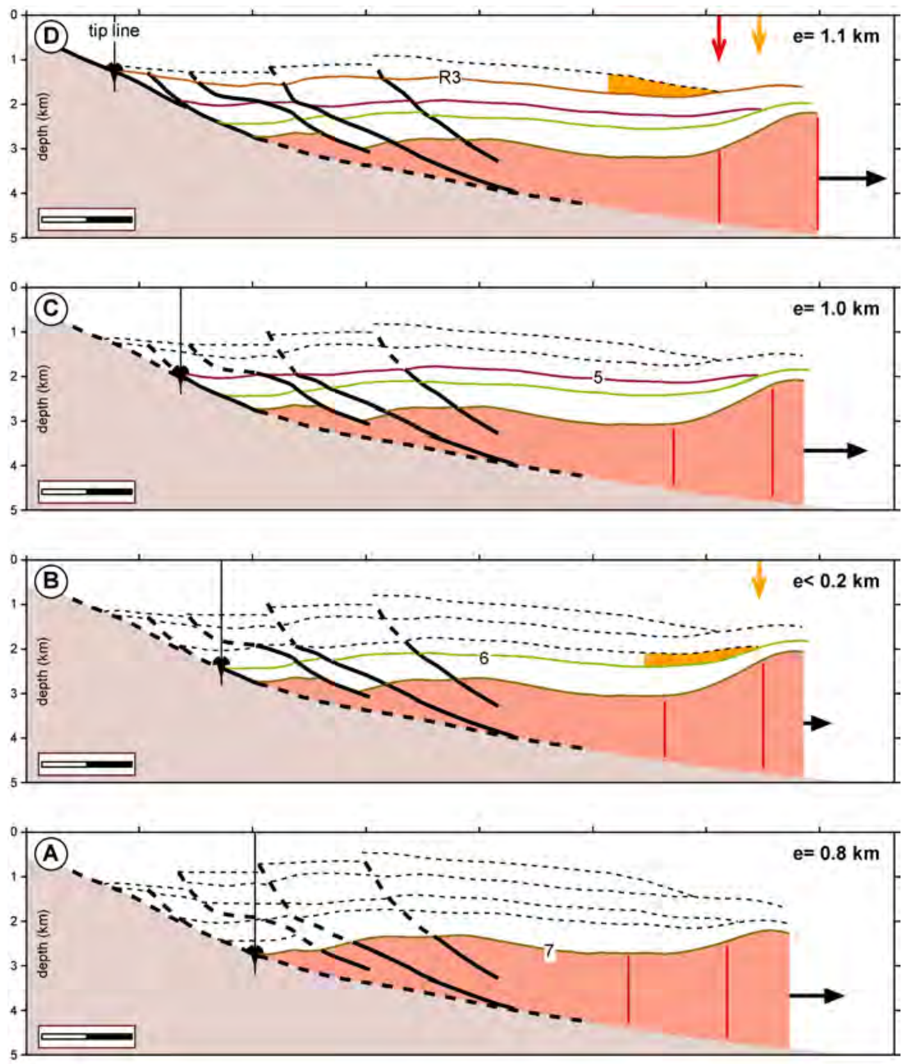

Figure 4: Restoration of the EAS-30 profile (Fig. 2) for the middle-Miocene extensional faulting in the WAB (pre-R3) and relationships with simultaneous mud-ascent episodes. Key-reflector codes as in Fig. 2. Vertical red bars are drawn to illustrate the possible horizontal motion within the mud diapir as a result of the horizontal extension driven by listric normal faulting. Scale bar corresponds to 2 km.

contrary, the final geometry of the sedimentary layer would depend on the balance between sedimentation rate and diapir vertical growth (Fig. 3b and 3c). In this case, when sedimentation rate surpasses the diapir ascent rate, the sedimentary units at the marginal troughs will decrease continuously in thickness towards the mud diapir culminations (Fig. 3b), or when opposite, they will eventually run into the diapir walls developing pinch-out geometries (Fig. 3c). These geometrical predictions can be also used to estimate the magnitude of the vertical ascent rate of the mud diapirs, comparing the sedimentary thicknesses between marginal troughs and at diapir culminations (Fig. 3b).

Low-angle, listric faults coalescing with the top-of-the-basement surface were formed and grew during this episode (Fig. 4), and forced the horizontal migration of the lowermost sediments toward the deeper segment of the basin. Down-slope mud migration occurred along the basement surface and was laterally stopped by a major residual basement high. Major episodes of mud diapir rise occurred concomitantly to normal faulting pulses and probably along antithetic normal faults. A complex pattern of triaxial strain with two simultaneous stretching directions (WSW-ESE and NNW-SSE) determined the diapir growth along these two main, orthogonal directions.

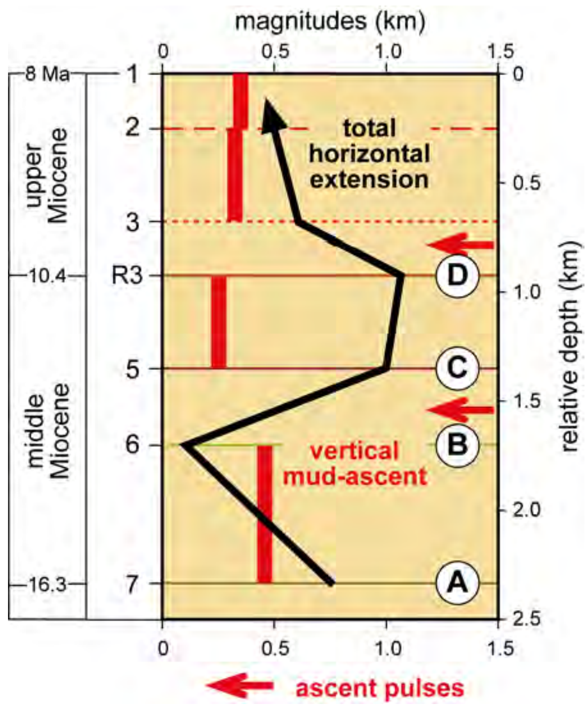

Figure 5: Temporary evolution during the middle and upper Miocene of the mud ascent episodes and the total horizontal extension estimated in the WAB with the seismic section shown in Fig. 2 (vertical and horizontal magnitude in km). Encircled letters correspond to restorations shown in Fig. 4 and color codes for the reflectors as in Figs. 2 and 4.

The magnitude of horizontal extension has been estimated in depth-converted seismic lines of the WAB (e.g. Fig. 4), based on the sequential restoration of the displacement along individual faults. Under these reconstructions, we have assumed no internal deformation of the fault blocks during or after faulting. With these assumptions, the extension estimates should be taken as a maximum value for the extensional deformation. These horizontal extension estimates should be also taken with caution, because for most of the faults we cannot reconstruct in three-dimensions the real fault heave or the hanging wall sense of displacement.

Mud ascent episodes during the middle-to-upper Miocene are closely related to extensional faulting (Fig. 5). We find mud ascent pulses during this period either under decreasing (e.g. between horizons 6 and 7) or increasing horizontal extension rates (e.g. between horizons 5 and R3). Nevertheless, the more striking pulses of diapir growth seem to occur immediately after or before major faulting episodes, namely in the middle Miocene (between horizons 7 and 6) or in the lowermost upper Miocene (between horizons R3 and 3), respectively. We could confirm from the WAB that subsurface mud-migration to feed diapirism growth is therefore linked to horizontal extension, although it tends to occur delayed with respect to major faulting episodes.

Mud diapirism and volcanism resume up to Present:

Late Miocene henceforth, diapir rise continued preferentially through the junctions between diapir culminations, meanwhile the WAB is under sub meridian contraction and roughly E-W transtension. Recently discovered mud volcanoes in the Spanish and Moroccan margins of the WAB, evidences that diapirism is still active in the Alboran Sea.

Mud diapirism evolved occurred during the Pliocene to Recent simultaneously with sedimentation, determining the local uplift, subsequent erosion, and thinning of the nearby coeval sedimentary units, producing local strata unconformities. Maximum thickness achieved at the border of the diapirs and the change in thickness around diapirs indicates that mud ascent followed existing fault surfaces. Sedimentary wedges, in the peripheral troughs, pinch out in opposite directions, evidencing the differential activation of the diapirs as well as their periodic ascent. The angular unconformities at the base of different Quaternary sub-units and their highly variable thickness suggest that there were at least two major pulses of diapir rise in the WAB during the late Pliocene and Quaternary (Talukder *et al.* in press).

While some diapirs stopped rising in the Pliocene-Quaternary and developed collapse structures in their tops, others resumed their ascent, with some reaching the seafloor connecting with active mud volcanoes. Volume loss by subsurface mud migration and fluid escape by extrusion are the most plausible causes for diapir collapse. The differential activation of the neighboring diapirs supports the participation of subsurface mud migration in the diapirism that occurred roughly perpendicular to the regional, maximum compressive stress (NNW-SSE). We propose that pulses of contractional deformation, coexistent with continuous subsidence and sediment overburden in the basin, may have repeatedly triggered mud diapirism and associated mud volcanism during the Pliocene to Recent.

References:

Barber, Tjokrosapoetro, and Charlton, 1986. American Association of Petroleum Geologists Bulletin, 70, 1729-1741.
Bishop, 1978. American Association of Petroleum Geologists Bulletin, 62, 1561-1583.
Bourgois, Mauffret, Ammar, and Demnati, 1992. Geo-Marine Letters, 12, 117-122.
Brown, 1990. Journal of Geophysical Research, 95, 8969-8982.
Camerlenghi, Cita, Hieke, and Ricchiuto, 1992. Earth and Planetary Science Letters, 109, 493-504.
Campillo, Maldonado, and Mauffret, 1992. Geo-Marine Letters, 12, 165-172.
Chalouan, Saji, Michard, and Bally, 1997. American Association of Petroleum Geologists Bulletin, 81, 1161-1184.
Cita, Erba, Lucchi, Pott, van der Meer, and Lieto, 1996. Marine Geology, 132, 131-150.
Comas, and Soto, 1999. Proceeding Ocean Drilling Program, Scientific Results, 161, 331-344.
Comas, García-Dueñas, and Jurado, 1992. Geo-Marine Letters, 12, 157-164.
Comas, Platt, Soto, and Watts, 1999. Proceeding Ocean Drilling Program, Scientific Results, 161, 555-579.
Comas, Soto, and BASACALB cruise (TTR-9 Leg 3). Intergovernmental Oceanographic Commission (UNES-CO), Workshop Report No. 168, 29-30.
Dewey, Helman, Turco, Hutton, and Knott, 1989. Geological Society of London, Special Publication, 45, 265-283.
Fowler, Mildenhall, Zalova, Riley, Elsley, Desplanques, and Guliyev, 2000. Journal of Petroleum Science and Engineering, 28, 189-206.
Fusi, and Kenyon, 1996. Marine Geology, 132, 21-38.
García-Dueñas, Balanyá, and Martínez-Martínez, 1992. Geo-Marine Letters, 12, 88-95.
Hedberg, 1974. American Association of Petroleum Geologists Bulletin, 58, 661-673.
Higgins, and Saunders, 1974. Verhandlungen der Naturforschenden Gesellschaft Basel, 84, 101-152.
Hovland, Hill, and Stokes, 1997. Geomorphology, 21, 1-15.
Jackson, and Vendeville, 1994. Geological Society of America Bulletin, 106, 57-73.
Jurado, and Comas, 1992. Geo-Marine Letters, 12, 129-136.
Kopf, Robertson, and Volkmann, 2000. Marine Geology, 166, 65-82.
Limonov, Woodside, Cita, and Ivanov, 1996. Marine Geology, 132, 7-19.
Maldonado, Campillo, Mauffret, Alonso, Woodside, and Campos, 1992. Geo-Marine Letters, 12, 179-186.
Martin, and Kastner, 1996. Journal of Geophysical Research, 101, 20325-20345.
Martínez-Martínez, Soto, and Balanyá, 1997. Terra Nova, 9, 223-227.
Martínez-Martínez, Soto, and Balanyá, 2002. Tectonics, 21/3, 3-1 - 3-22.
Pérez-Belzuz, Alonso, and Ercilla, 1997. Tectonophysics, 282, 399-422.
Platt *et al.*, 2003. Tectonics, 22-3.
Reed, Silver, Tagudin, Shiley, and Vrolijk, 1990. Marine and Petroleum Geology, 7, 44-54.
Robertson, and Shipboard Scientific Party 1996. Geology, 24, 239-242.
Sautkin, Talukder, Comas, Soto, and Alekseev, 2003. Marine Geology, 195, 237-261.
Soto, Comas, and de la Linde, 1996. Geogaceta, 20, 382-385.
Talukder, Comas, and Soto, 2003. Special Publication of the Geological Society of London, in press.
Vendeville, and Jackson, 1992. Marine and Petroleum Geology, 9, 331-353.
Watts, Platt, and Buhl, 1993. Basin Research, 5, 153-177.
Wiedicke, Neben, and Spiess, 2001. Marine Geology, 172, 57-73.